1 **Snow algae communities in Antarctica - metabolic and taxonomic**

2 **composition**

3

4 **Matthew P. Davey[1][*](ORCID: 0000-0002-5220-4174)**

5 **Louisa Norman[1]**

6 **Peter Sterk[2] (ORCID: 0000-0003-1668-7778)**

7 **Maria Huete-Ortega[1] (ORCID: 0000-0002-8746-5518)**

8 **Freddy Bunbury[1]**

9 **Bradford Kin Wai Loh[1] (ORCHID: 0000-0002-7762-8539)**

10 **Sian Stockton[1]**

11 **Lloyd S. Peck[3]**

12 **Peter Convey[3] (ORCHID: 0000-0001-8497-9903)**

13 **Kevin K. Newsham[3] (ORCHID: 0000-0002-9108-0936)**

14 **Alison G. Smith[1] (ORCHID: 0000-0001-6511-5704)**

15

16 [1]Department of Plant Sciences, University of Cambridge, Cambridge, CB2 3EA,

17 UK

18 [2]Cambridge Institute for Medical Research, University of Cambridge, Wellcome

19 Trust MRC Building, Hills Road Cambridge, CB2 0QQ, UK

20 [3]British Antarctic Survey, NERC, Madingley Road, Cambridge, CB3 0ET, UK

21 *Corresponding author: mpd39@cam.ac.uk Tel: +44(0)1223 333943

22 **Twitter account: @scienceisnotfun   @plantsci**

23

32

Summary:

- Snow algae are found in snowfields across cold regions of the planet, forming highly visible red and green patches below and on the snow surface. In Antarctica, they contribute significantly to terrestrial net primary productivity due to the paucity of land plants, but our knowledge of these communities is limited. We hence provide the first description of the metabolic and species diversity of green and red snow algae communities from four locations in Ryder Bay (Adelaide Island, 68°S), Antarctic Peninsula.

- During the 2015 austral summer season, we collected samples to measure the metabolic composition of snow algae communities and determined the species composition of these communities using metabarcoding.

- Green communities were protein-rich, had a high chlorophyll content and contained many metabolites associated with nitrogen and amino acid metabolism. Red communities had a higher carotenoid content and contained more metabolites associated with carbohydrate and fatty acid metabolism. *Chloromonas*, *Chlamydomonas* and *Chlorella* were found in green blooms but only *Chloromonas* was detected in the red blooms. Both communities also contained bacteria, protists and fungi.

- These data show the complexity and variation within snow algae communities in Antarctica and provide initial insights into the contribution they make to ecosystem functioning.

Introduction:

Terrestrial life in Antarctica is largely found on the estimated 0.18% of the continent's surface that is ice-free for at least part of the year (Convey, 2017; Burton-Johnson *et al*., 2016). But even here, only a small proportion of this exposed area is vegetated. For example, although the Antarctic Peninsula is the most vegetated region of Antarctica, only 1.34% of exposed ground has plant cover (Fretwell *et al*., 2011; Burton-Johnson *et al*., 2016). However, the actual area of cover by autotrophs may be much higher, as ground-truthing of satellite imagery has revealed that in many places vegetation comprises not only patches of bryophytes, lichens and higher plants on exposed ground, but also snow algae. Snow algae blooms are often well developed in coastal snowfields as highly visible red and green patches below and on the snow surface where liquid water is present (Fogg, 1967; Broady, 1986; Müller *et al.,* 1998). Many snow algal communities consist of either a vegetative stage, seen as green patches in the snow, with *Chloromonas* and *Chlamydomonas* species frequently being the major algal taxa, or an encystment phase (which may also be vegetative), in which the cells have accumulated the keto-carotenoid astaxanthin, giving rise to red snow patches (Hoham & Duval, 2001; Komárek & Nedbalová, 2007; De Wever *et al*., 2009; Leya, 2013). Fretwell *et al*. (2011) found that areas of snow algae and terrestrial mats in Antarctica could be identified in satellite images in combination with ground-truthing. If these measurements are typical of terrestrial communities more widely in Antarctica, and considering that a single snow algal 'bloom' on the peninsula can cover tens to hundreds of square metres, snow algae are potentially one of the region's most significant photosynthetic primary producers, substantially increasing the known area of land occupied by primary producers in Antarctica. Furthermore, the contribution made by snow algae to terrestrial ecosystem productivity in the Antarctic is likely to be higher than that in the Arctic and other alpine regions, since algal blooms in these other regions tend to be more patchy and occur close to other well-established and extensive vegetated areas. More widely, these algae play a key role in nutrient dynamics, assimilating nutrients deposited from bird colonies which, as a result of snow-melt, are leached with their associated microbial community into adjacent

97   terrestrial or marine environments, where they support food chains (Dierssen *et*
98   *al*., 2002; Hodson *et al*., 2008; Boetius *et al*., 2015). Significantly, recent studies
99   of snow algae in the High Arctic have shown that they can alter the albedo of the
100   snow, with darker snow surfaces during red phase algal blooms increasing the
101   local rate of snow melt (Lutz *et al*., 2016; Cook *et al*., 2017; Ganey *et al*., 2017;
102   Stibal *et al*., 2017).

103   The Antarctic Peninsula has an extremely variable climate. The region
104   experienced a strong warming period throughout the second half of the twentieth
105   century that resulted in increased snow melt, and at present is undergoing a
106   period of temporary cooling (Turner *et al*., 2009, 2016). Climate warming along
107   the Antarctic Peninsula has resulted in an increase in growing season
108   temperature as well as the availability of water, meaning that two of the major
109   abiotic constraints on biological activity have been relaxed. This may well result
110   in an extended growing season (Vaughan, 2006; Convey, 2011; Chown &
111   Convey, 2012). Thus, there is a potentially large increase in the duration of the
112   algal bloom season associated with a warmer climate in the region. Conversely,
113   cooler periods with a shift in the general wind direction could see the current
114   habitat for snow algae preserved. With habitat regression, or if areas of snow
115   melt completely early in the summer, the ecosystem may be lost entirely for that
116   season (Convey, 2011; Anesio *et al*., 2017). Whichever outcome prevails - which
117   is likely to vary with location - there is an urgent need to study these polar
118   communities to provide a balanced view of polar terrestrial biodiversity and to
119   avoid the loss of these extremophilic primary producers and their community
120   structure at both local and continental scales (Williams *et al*., 2003; Rogers *et al*.,
121   2007; Hamilton & Havig 2017; Rintoul *et al*., 2018). This is especially pertinent
122   as, although snow algae may not be endemic, there is evidence of endemism
123   and long-term evolutionary isolation in other associated microbial species and
124   communities around Antarctica, likely due to the geographical isolation of the
125   continent (Petz *et al*., 2007; Vyverman *et al*., 2010; Remias *et al*., 2013;
126   Cavicchioli *et al*., 2015).

127   Despite the ecological importance of Antarctic snow algae, our knowledge
128   of their diversity, distribution, growth and contribution to nutrient cycles is limited

129   to very few locations, such as Goudier Island (64°49'S, 63°29'W) and Paradise
130   Harbour (64°50'S, 62°52'W) (Remias *et al.*, 2013). It is currently unknown how
131   prevalent snow algae are in Antarctica, and how much they contribute to primary
132   productivity. Determining the abundance of snow algae will therefore enhance
133   and balance our understanding of the biodiversity of Antarctica. In this study, our
134   objective was to carry out the first estimate of the metabolic and species diversity
135   of snow algae communities collected from four islands in Ryder Bay, adjacent to
136   the Antarctic Peninsula. Specifically, we set out to test whether green and red
137   algae communities have distinct metabolic profiles beyond visual differences in
138   pigmentation. To this end, we investigated the metabolic similarities and
139   differences between green and red blooms in Ryder Bay to identify key shifts in
140   the functional biochemistry of the organisms, the spatial variability of the
141   metabolic composition of snow algae communities and the taxonomic diversity of
142   the communities, in order to identify the algae present and to determine the
143   identity and composition of associated bacterial, protist and fungal communities.
144   To ensure that a wide range of metabolites were detected and identified at this
145   exploratory stage, we used both targeted and untargeted environmental
146   metabolomic approaches in the field (FT-IR) (to ensure minimal sample
147   degradation) and in the laboratory (HPLC, GC-FID, GC_MS) (Bundy *et al.*, 2009;
148   Brunetti *et al.*, 2013). To assess the quantity of the metabolites in the
149   environment, data were expressed on a per litre of snow melt basis as well as
150   per unit of dry cell mass. We also used a 16S rRNA gene and ITS metabarcoding
151   approach to determine the species composition of the microbial community in the
152   snow algae blooms.
153
154   **Methods:**
155   **Field collections in Antarctica:** Snow algae communities (Fig. **1**) were collected
156   in 6 x 50 ml sterile plastic sample tubes from layers of green and red dominant
157   snow algal blooms at four locations in Ryder Bay, Antarctic Peninsula (Rothera
158   Point, Anchorage Island, Léonie Island and Lagoon Island) in austral summer
159   (Jan–Feb) 2015 (Table **S1**). It was not possible to determine whether all blooms
160   surveyed were successional stages or distinct assemblages. The layers of algae

161   were 1–5 cm deep, but with much heterogeneity within a bloom, with only the

162   algae layer sampled in that 1-5cm depth. The algae were collected by filling a

163   sterile 50 ml tube with snow, which was not compacted. Seven blooms were

164   studied at Rothera Point (42 samples), nine at Anchorage Island (54 samples),

165   five at Léonie Island (30 samples) and 10 at Lagoon Island (60 samples),

166   resulting in 186 samples for subsequent analyses. Blooms lasted for at least 42

167   d with bloom areas ranging from approximately 5 m^2 to >2500 m^2. Single point

168   photosynthetically active radiation (PAR) (Skye PAR Quantum Sensor, Skye

169   Instruments Ltd., Powys, UK) received at the snow surface, together with

170   temperature measurements (standard glass thermometer) at the snow surface

171   and 5 cm depth were also recorded at the start of each sampling period, which

172   lasted for 30–60 min). Samples were returned within 3 h of sampling to the

173   Bonner Laboratory (Rothera Research Station, Ryder Bay, Antarctica), where

174   they were melted in 4 °C lit incubators (Sanyo). Algal cell density was measured

175   by adding 6 µl of snowmelt into Hycor Kova® haemocytometer wells and counting

176   the number of algal cells using bright field microscopy. Algal community dry cell

177   mass was obtained by gravity filtration of 50 ml of melted snow through a pre-

178   weighed dry filter (Whatman GF/C, 47 mm). Filters were dried at 80 °C for at least

179   48 h prior to re-weighing. Samples for FT-IR analysis, which enabled

180   measurements to be obtained as close as possible to the time of sampling

181   ensuring minimal metabolic degradation, were processed by pelleting 2 ml of

182   snowmelt (2000 g for 10 min at 4 °C), discarding the supernatant and drying the

183   pellet at 80 °C for 24 h, followed by 24 h in a desiccator. The dried pellets were

184   analysed on station using a Perkin-Elmer Spectrum Two FT-IR, set to measure

185   the absorbance intensity between wavenumbers 400 to 4000 cm^{-1} and

186   normalised against air. For the metabolite and genomic analysis, carried out at

187   the Department of Plant Sciences, Cambridge, 10 ml of snow melt was pelleted

188   using centrifugation (2000 g for 10 min, 4 °C), after which the supernatant was

189   discarded and the remaining algal pellet was flash frozen in liquid nitrogen and

190   stored at -80 °C. Live algae were transported to the UK by adding 20 µL of

191   snowmelt containing algae onto Tris-Acetate-Phosphate (TAP) agar slopes in 30

192   ml clear plastic tubes for growth under controlled conditions (4 °C, 10 µmol m^2 s^{-1}

193   12:12 hours light:dark cycle) at Cambridge and were imported under UK

194   APHA/DEFRA license number 119979/260872/0. The slopes and frozen

195   samples were transferred to the UK by ship at 4 °C or -80 °C.

196

197   **Pigment analysis:** Total chlorophyll and carotenoid concentrations were

198   determined after extraction of pigments from cell pellets (from 1 ml snowmelt)

199   with 1 ml dimethylformamide using the equations of Inskeep & Bloom (1985) and

200   Wellburn (1994). Individual pigments were analysed by HPLC by first adding 1

201   ml deionised water to resuspend the pelleted cells. The resuspended pellets were

202   transferred to a 2 ml microfuge tube and re-pelleted (16,000 g for 10 min). The

203   supernatant was removed and the remaining pellet homogenised with glass

204   beads and frozen in liquid nitrogen three times, after which 1 ml of

205   dimethylformamide was added and sonicated for 30 min. Samples were re-

206   pelleted and the supernatant transferred to an HPLC glass vial, mixed with

207   methanol (3:2) and stored at -80 °C until analysis. Pigments were separated by

208   HPLC (Surveyor system, Thermo Scientific, San Jose, CA, USA) as described

209   by Remias & Lütz (2007) but using an injection volume of 50 µl, and were

210   resolved on a Luna C18 column (250 x 2.0 mm, Phenomenex, Macclesfield, UK).

211   Peaks were compared against standards (astaxanthin and astaxanthin esters,

212   lutein, chlorophyll a and chlorophyll b, and β-carotene) (Inskeep & Bloom 1985;

213   Wellburn 1994), purchased from Sigma Aldrich.

214

215   **Total cellular lipids and FAMEs:** Lipids were extracted using the

216   chloroform/methanol/water method and triacylglycerides (TAGs), polar lipids and

217   free fatty acids in the total lipid extract and total fatty acid methyl esters (FAMEs)

218   were analysed by gas chromatography, as described in Davey *et al*. (2014).

219

220   **Metabolite profiling:** Soluble polar and non-polar metabolites were extracted

221   using the methanol-chloroform-water method as described in Davey *et al*. (2008).

222   Compounds within the polar methanol-water phase were derivatised by N-

223   Methyl-N-trimethylsilyl-trifluoroacetamide (MSTFA) and Trimethylsilyl (TMS) as

224   described by Dunn *et al*. (2011) and subsequently separated and profiled by GC-

225   MS (Thermo Scientific Trace 1310 GC with ISQ LT MS, Xcaliber v2.2) with a ZB-

226   5MSi column (30 m, 0.25 mm ID, 0.25 μm film thickness, Phenomenex, UK). The

227   injection volume was 1 μl (splitless) with an injector temperature of 300 °C, using

228   helium as a carrier gas (constant flow rate of 1.0 ml min^{-1}). The following gradient

229   was used: initial oven temperature 70 ºC; 130 ºC at 10 ºC min^{-1}; 230 ºC at 5 ºC

230   min^{-1}; 310 ºC at 20 ºC min^{-1}; hold for 5 mins. The mass spectrometry conditions

231   in the positive mode were: transfer line 310 ºC; ion source, 310 ºC; mass range

232   45-800 Da; dwell time 0.17 amu/s. GC-MS spectra were aligned to an internal

233   standard (phenyl-β-d-glucopyranoside hydrate 98%, Davey *et al*., 2008) and

234   processed using Thermo Tracefinder (v3.1) and NIST software (NIST v2.0

235   http://www.nist.gov/srd/nist1a.cfm) to aid identification based on molecular mass.

236   Pathway analysis of the identified metabolites used MetaboAnalyst open source

237   software (v4, pathway analysis tool) using the *Arabidopsis thaliana* metabolic

238   pathway library (Chong *et al*., 2018, www.metaboanalyst.ca). R-script for the

239   metaboanalyst software can be downloaded at https://github.com/xia-

240   lab/MetaboAnalystR (Chong & Xia, 2018).

241

242   **Metabarcoding:** Frozen pellets (approximately 1cm^3) of field-collected algal

243   communities from 10 ml snow melt were allowed to thaw before being

244   resuspended in 1 ml of RNase-free water. After transferring to a clean 1.5 ml

245   microfuge tube, the samples were ground with sterilised sand before adding

246   another 1 ml of RNase-free water and subsequent transfer to a 15 ml capacity

247   tube to which 3 ml of SDS-EB buffer (2% SDS, 400 mM NaCl, 40 mM EDTA, 100

248   mM Tris-HCl, pH8.0) were added, followed by mixing by vortexing and shaking

249   for 5 min at 4 °C. Subsequently, 3 ml of chloroform were added, mixed gently by

250   inversion and the whole suspension was centrifuged for 5 min at 2000 *g* and 4

251   °C, resulting in a two phase separation. The top aqueous phase was transferred

252   to a new 15 ml capacity tube and two volumes of 100% chilled ethanol were

253   added before incubating overnight at -20 °C. The following day, the mix was spun

254   at 6800 *g* at 0 °C for 30 min. After carefully discharging the supernatant, the pellet

255   was resuspended with 1 ml of ethanol (70%) and recovered in a clean microfuge

256   tube before determining total RNA concentration and quality. Libraries of the

257 fourth hypervariable (V4) domain of 16S rRNA gene and internal transcribed

258 spacer region (ITS) of rRNA gene were produced using the NEXTflex™ "16S V4"

259 and "18S ITS" Amplicon-Seq Library Prep Kit and primers (BIOO Scientific,

260 Austin, TX), respectively. For consistency we hereafter use the term "ITS" for the

261 NEXTflex 18S-ITS region. The microbial 16S rRNA gene forward primer (V4

262 Forward) sequence was: 5'-

263 GACGCTCTTCCGATCTTATGGTAATTGTGTGCCAGCMGCCGCGGTAA-3'

264 and   the   reverse   primer   (V4   Reverse)   sequence   was: 5'-

265 TGTGCTCTTCCGATCTAGTCAGTCAGCCGGACTACHVGGGTWTCTAAT-3'.

266 The eukaryotic ITS forward primer (18S ITS Forward) sequence was: 5'-

267 CTCTTTCCCTACACGACGCTCTTCCGATCTTCCGTAGGTGAACCTGCGG-3'

268 and   the   reverse   primer   (18S   ITS   Forward)   5'-

269 CTGGAGTTCAGACGTGTGCTCTTCCGATCTTCCTCCGCTTATTGATATGC-

270 3'. Samples were sequenced by Cambridge Genomic Services (Cambridge, UK)

271 using an Illumina MiSeq v3 600-Cycle Sequencer following the manufacturer's

272 protocol and primers. Quality control analysis of the Illumina MiSeq paired-end

273 reads   (2x300   bp)   was   performed   using   FastQC

274 (https://www.bioinformatics.babraham.ac.uk/projects/fastqc/).   Taxonomic

275 analysis of 16S rRNA gene sequences was performed using QIIME 2 release

276 2017.10 (Caporaso *et al*., 2010; https://qiime2.org). In brief, for each sample,

277 demultiplexed paired end sequences were imported into QIIME2. Potential

278 amplicon sequence errors were corrected with the QIIME 2 implementation of

279 DADA2 (Callahan *et al*., 2016). In order to remove lower quality bases, reads

280 were truncated at position 280 based on the FastQC reports during this step.

281 Taxonomy was assigned to the sequences in the feature table generated by

282 DADA2 using Silva release 128 as 16S/ITS(18S) marker gene reference

283 database (Quast *et al*., 2013), trimmed to the V4 region, bound by the 515F/806R

284 primer pair used for amplification. Taxonomic analysis of the ITS sequence data

285 was done as described for the 16S rRNA gene up to the taxonomic assignment

286 step. Because of the lack of an ITS marker reference database representative of

287 the species diversity of the environments investigated, we carried out sequence

288 similarity searches using NCBI BLAST (Altschul *et al*., 1990) against release 134

289   of the European Nucleotide Archive. Taxonomic assignments were made

290   manually, based on blast scores and the presence or absence of ambiguity of the

291   taxonomic lineages reported by BLAST. For ambiguous BLAST hits (e.g. a similar

292   score for unrelated taxa), the lowest common denominator was used for

293   taxonomic assignment. Since there were so few OTUs, and in the absence of an

294   ITS database that is representative of the communities under investigation, we

295   treated these results as exploratory. Sequence reads were submitted to the

296   European Nucleotide Archive (ENA) Sequence Read Archive at the European

297   Bioinformatics Institute (https://www.ebi.ac.uk/ena) and are available under

298   accession number PRJEB23732.

299

300   **Targeted 18S rRNA gene PCR for isolated snow algae species:** Snow algae

301   were isolated from a field sample (Lagoon Island) and grown axenically on TAP

302   agar plates supplemented with ampicillin (50 µg ml^{-1}) and kasugamycin (50 µg

303   ml^{-1}). Cultures were maintained under a 12:12 light:dark photoperiod at 4 °C. PCR

304   reaction mixtures contained REDTaq ReadyMix PCR Reaction Mix (Sigma) with

305   10 µM of the 18S rRNA gene universal eukaryotic primers (Forward sequence

306   "SA Forward": 5'-CGGTAATYCCAGCTCCAATAGC-3', Reverse sequence "SA

307   Reverse": 5'-GTGCCCTTCCGTCAATTCC-3'), expected product size: 582–584

308   bp. Primers were adapted from Wang *et al*. (2014) where our forward primer was

309   a 3' section of the first primer in their Table 1, with the addition of nucleotides

310   downstream of it so the primers would have similar annealing temperatures,

311   avoiding a run of guanines and cytosines and to avoid the possibility of forming

312   stable secondary structures or primer dimers. Our reverse primer is the reverse

313   complement of a section of the second listed primer in their Table 1. The PCR

314   reaction cycle was 95°C 5 min, 95°C 20 s, 55° 20 s, 72° 1 min (35 cycles), 68° 5

315   min. PCR products were extracted from the gel using a QIAquick Gel Extraction

316   kit (QIAGEN), following the manufacturer's instructions and nucleotide

317   sequencing (both directions using the above primers) was performed using

318   Applied Biosystem sequencing platforms (Abi 3730xl genome analyser, 50cm 96

319   capillary array) at Source BioScience (Cambridge, UK) and viewed using

320   Snapgene v4.2.4. Nucleotide sequences were deposited at GenBank and are
321   available under accession numbers MK330877-MK330880.

322

323   **Statistics:** To determine whether the differences between green and red
324   communities, or among bloom site locations, were statistically significant, *t*-tests
325   (Excel, Microsoft Office 2007) or two-way ANOVA with Tukey's test (SigmaPlot
326   v13.0, Systat Software Inc. CA, USA) were performed. Multivariate analyses to
327   test whether green and red communities could be discriminated based on their
328   identified and unidentified metabolites (from FT-IR fingerprints or GC-MS profiling
329   datasets) were performed using Principal Component Analysis (PCA) (Paliy &
330   Shankar 2016) on Unit-Variance Scaled data (FT-IR absorbance values or GC-
331   MS identified peak area units) within the Simca-P v14.1 PCA analysis pipeline
332   (Umetrics, Sweden) to produce standard score scatter plots and ranked score
333   contribution plots of how each variable (FT-IR wavenumber or GC-MS
334   metabolite) contributed to clustering within the PCA score scatter plot.
335   Alpha diversity and beta diversity were measured using QIIME 2's diversity
336   analyses   [q2-diversity]   plugin   (version   2017.10;
337   https://docs.qiime2.org/2017.10/tutorials/moving-pictures/). In brief, the core-
338   metrics-phylogenetic method was applied, which first subsamples the counts
339   from each sample in order to obtain an even sampling depth (43828 for the 16S
340   rRNA data and 69 for the ITS data). Alpha and beta diversity metrics (Faith's
341   Phylogenetic Diversity and Pielou's Evenness) were subsequently computed
342   (PERMANOVA). To determine whether the richness of the samples had been
343   fully captured, alpha diversity rarefaction plots were calculated using the QIIME
344   diversity alpha-rarefaction visualizer. Plots for 16S rRNA gene and ITS data
345   approached saturation at depths of 43828 and 69 sequences, respectively (Fig.
346   **S1**), suggesting that the majority of the diversity in the communities had been
347   captured. Beta diversity non-metric multidimensional scaling (NDMS) plot
348   analysis of the raw read metabarcoding data was carried out using R script in
349   vegan (Supporting Methods **S1**; https://jonlefcheck.net/2012/10/24/nmds-
350   tutorial-in-r/) with stress levels of 0.1–0.2, using the Bray-Curtis dissimilarity
351   calculation (Paliy & Shankar 2016). Given the limited access to some blooms,

352 and to reduce the environmental impact, the sample numbers (n) varied (1 to 30)

353 per site, as such sample numbers are given in the figure and table legends.

354

355 **RESULTS:**

356

357 ***Algal community cell density and biomass***

358 There were many fewer cells in the red algal communities than in the green

359 communities, with mean (± S.D.) cell densities of 0.15×10^6 cells per ml snow

360 melt (± 0.17×10^6) versus 1.24×10^6 cells per ml snow melt (± 0.79×10^6)

361 respectively (Fig. **S2a**). Similarly, the two communities differed in dry biomass

362 (mg l^{-1} of snow melt), with, on average across all sites, 62% less biomass in the

363 red-dominated communities than in the green communities (Fig**. S2b**). There

364 were no significant differences (ANOVA $P > 0.05$) in cell numbers or cell dry

365 masses between sampling locations in the red communities. However, the green

366 communities on Léonie Island had a greater number of cells (~2.2×10^6 more

367 cells per ml) and biomass (~2.9 g dry mass more per l) of snow melt than on the

368 other islands (ANOVA, $P \leq 0.01$).

369

370 ***FT-IR metabolite fingerprinting***

371 Fourier Transform-Infrared Spectrometry (FT-IR) was used during the field

372 campaign to analyse the metabolic composition of the snow algae communities

373 as close to field conditions as possible (Fig. **2a**). Based on principal component

374 analysis (PCA), there were specific FT-IR wavenumber regions that were strongly

375 associated with green (1489–1581, 1589–1664 cm^{-1}) or red (1002–1094, 1141–

376 1144, 1732-1756, 2850-2856, 2911-2933 cm^{-1}) snow algae communities (Fig.

377 **2b**). These regions were associated with protein bands (amide I and II) -

378 suggestive of active growth - in the green communities, whereas in red

379 communities the major features were associated with lipids, lipid esters and

380 polysaccharides (Fig. **2b**, Table **S2**). There was no clustering of samples based

381 on sample island location. Little variation across island locations suggests that

382 the sampling regime was standardised and robust.

383

Pigments composition in snow algae blooms

Crude solvent extractions and UV-Vis spectrometry of green and red blooms shortly after field collection showed the presence of peaks indicative of chlorophyll *a* and *b* and astaxanthin (Fig. **S3**). There were significant differences in the total chlorophyll content of green and red dominant snow algae communities, with more total chlorophyll present in the green than in the red communities when expressed on a per unit dry mass (~83% more) and per volume snow melt (~90% more) (Fig. **S4a,b**). There was no difference in the concentrations of total carotenoid between the red and green blooms, when expressed either on a per unit dry mass basis (Fig. **S4c**) or per l of snow melt (Fig. **S4d**) basis. There was a single effect of location, with the chlorophyll content of the Léonie Island green community having more chlorophyll per unit of snow melt than the other islands ($P \leq 0.05$), which was probably due to the greater biomass per unit of snow melt at that location. There were no other effects of location on total chlorophyll or total carotenoid in the red communities.

Pigment composition was analysed in detail using HPLC. As there was minimal effect of location from the above pigment analyses, samples from the islands were pooled to provide an average composition over Ryder Bay for green and red communities (**Table 1**). Dominant pigments in the green community were chlorophyll *a*, *b*, β-carotene and lutein, and in the red community were chlorophyll *a*, *b* and astaxanthin esters. The main differences between the communities were that the red communities had significantly less chlorophyll *a* and *b*, β-carotene, lutein (*t*-test $P \leq 0.05$) and xanthophyll and more astaxanthin-like and astaxanthin esters, although these were not significant (**Table 1**). The ratio of chlorophyll *a*:*b* was similar in both green (1.9:1) and red (2.2:1) communities.

Lipid profiling of green and red blooms

More detailed analyses using GC-FID and GC-MS were performed in order to qualify and quantify differences between communities identified from FT-IR spectra. We first measured the overall glycerolipid composition of the samples (expressed as mg per unit dry cell mass). Unlike the other metabolites detected, there was little variation in the non-polar (TAG) and polar lipid content between

416   the green and red communities, nor between the different island locations. The

417   exception to this was significantly ($P \leq 0.05$) more neutral storage lipids (TAGs)

418   per unit dry mass in the lipid extracts from the red community at Lagoon Island

419   (Fig. **3a**). A significantly higher concentration of free fatty acids was also

420   measured in the red communities from Léonie Island (Fig. **3e**). However, when

421   data were expressed per litre of snow melt, the polar membrane lipid content of

422   the red community from Léonie Island was less than that of the green community

423   ($P \leq 0.01$; Fig. **3d**), and the mean free fatty acid concentration in the red

424   communities was lower compared to the green communities from all locations

425   except Lagoon Island ($P \leq 0.05$; Fig. **3f**). There were no significant differences in

426   lipid composition in either the red or green communities between the sampling

427   locations.

428   FAME analyses showed that the snow algae communities contained a

429   range of saturated and unsaturated fatty acids from C14:0 to C22:6 and were rich

430   in the saturated C16:0 and unsaturated C18:1(11) fatty acids (Table **S3**). Overall,

431   there were no statistically significant differences in the fatty acid profile between

432   the green and red communities, but the trend was for greater amounts of C16:0,

433   C18:1(11) and C18:1(9) fatty acids in the red community, and lower or similar

434   amounts of all other fatty acids.

435

436   ***Metabolic profiles of red and green snow algae communities***

437   To provide further insight into the metabolic composition of the different snow

438   algae communities, an untargeted metabolic profiling approach was used where

439   the extracts were derivatised by MSTFA, analysed by GC-MS and peaks

440   identified. PCAs showed distinct clustering of green and red communities (Fig.

441   **4a**). There was no clustering of samples based on island location in any of the

442   principal components. The score contribution of metabolites (based on their

443   molecular masses and comparisons with NIST MS libraries) and the metabolic

444   pathways in which they are involved were ranked in order of importance for either

445   green or red snow algae communities using an *in silico* MetaboAnalyst Pathway

446   Analysis Tool. Metabolites involved in energy production and the TCA cycle and

447   in nitrogen and amino acid metabolism, such as succinic acid and the amino acids

448　asparagine and valine, were strongly associated with green snow algae

449　communities (Fig. **4b,** Tables **S4 and S5**). The most frequent metabolites

450　associated with red communities were quite different from those in the green

451　communities. They were largely associated with osmolytes (mannitol, xylitol) and

452　the fatty acids heptadeconoic acid (an unsaturated C17 fatty acid) and dimethyl-

453　heptanoic acid (a C7 volatile acid).

454

455　***Snow algae community composition***

456　Bright-field microscopy revealed mainly flagellated and non-flagellated green

457　algal cells representing the vegetative stage in green blooms, and orange to red

458　mature zygospores or large hypnozygotes in red blooms (Fig. **S3**). Although

459　green algal blooms in Ryder Bay were observed to become red over periods of

460　about 30 d, given the remote location, which precluded many repeat samplings,

461　it could not be irrefutably established whether the red forms of the cells were

462　derived from the green vegetative cell forms, or if the red cells were a separate

463　assembly that succeeded green blooms.

464　　　　We therefore carried out metabarcoding analysis to investigate the

465　species composition of the communities, via sequencing libraries of the V4 region

466　of 16S rRNA gene and ITS region of each community and then by NMDS plot

467　analysis of the 16S rRNA gene or ITS OTUs. Both read frequencies and

468　percentage contributions were obtained for two major taxonomic levels

469　(Kingdom/Phylum Level 2 to Genus Level 7). To test for associations between

470　discrete metadata categories (green and red algae communities) and alpha

471　diversity data, the community richness and evenness were calculated using

472　Faith's Phylogenetic Diversity (a qualitative measure of community richness that

473　incorporates phylogenetic relationships between the features) and Pielou's

474　Evenness (a measure of community evenness). No significant differences in

475　community richness or evenness were measured between green and red 16S

476　rRNA gene and ITS sequence-based communities ($P \geq 0.05$, Kruskall-Wallis test)

477　(Fig. **S5**). For beta diversity, a PERMANOVA (Anderson 2001) test (using QIIME

478　2's beta-group-significance command) on unweighted UniFrac distances

479　generated during the first diversity analysis step was used to test whether

480   sequence reads from samples within a bloom type were more similar to each
481   other than they were to samples from the other bloom type. Similar to alpha
482   diversity, there was no significant dissimilarity between the green and red 16S
483   rRNA gene and ITS communities ($P \geq 0.05$) (Fig. **S6**). Beta diversity NMDS plots
484   of both 16S rRNA gene and ITS data sets also revealed close taxonomic
485   similarities between the green and red communities (Fig. **S7**).

486   Despite being the major observable organisms in the samples, the
487   Chlorophyta contribute little to the overall diversity, which was instead dominated
488   by fungi, other protists and bacteria (Fig. **5;** Tables **S6-S8**). However, of note is
489   the difference in the Chlorophyta between the green and red blooms: in the green
490   blooms OTUs whose closest hit in the databases were to *Chloromonas*,
491   *Chlamydomonas* and *Chlorella* were detected in approximately equal measures,
492   but in the red blooms, only *Chloromonas* was identified, with the other OTUs
493   being assigned to unknown Chlorophytes (Fig. **S8**), indicating that the red
494   community contains other, unidentified green algal species. Further investigation
495   into the identity of the snow algae in the red blooms, based on preliminary
496   analysis of their morphology, suggested that they could either be
497   *Chlamydomonas nivalis* or *Chloromonas nivalis*. To ascertain this, 18S rRNA
498   gene PCR was performed on nucleotide extracts from red snow algae cultures
499   that were isolated from a field sample (Lagoon Island) and grown axenically,
500   during which the cells transformed from their red phase to a green phase (over
501   21 d). A BLAST search of the forward and reverse nucleotide sequences resulted
502   in 98–99% similarity to *Chloromonas* sp. and *Chlamydomonas* sp., supporting
503   our initial classification. However, a BLAST search against only *Chlamydomonas*
504   *nivalis* or *Chloromonas nivalis* sequences resulted in just 92% similarity (Table
505   **S9**) indicating that these might be other species. At the class level, sequence
506   reads from the 16S rRNA gene metabarcoding showed that the communities
507   were dominated by *Flavobacteria*, *Sphingobacteria* and beta-proteobacteria, in
508   particular *Flavobacterium*, *Pedobacter* and *Hymenobacter*, respectively (Fig. **5a**).
509   The number of Sphingobacteria OTUs was found to be statistically significantly
510   lower ($P < 0.05$) and *Chryseobacterium* reads significantly higher ($P < 0.01$) in
511   the red communities compared to the green communities (Tables **S7-S8).**

512

513 **DISCUSSION:**

514 Our objective was to carry out the first estimate of the metabolic and species

515 diversity of snow algae communities collected from four islands in Ryder Bay,

516 adjacent to the Antarctic Peninsula. Our study demonstrates that green and red

517 Antarctic snow algae communities have unique biochemical profiles beyond the

518 observable differences in pigmentation and are members of complex microbial

519 communities that include a range of bacterial, protist and fungal taxa.

520

521 ***Metabolic composition differs between green and red snow algae blooms***

522 From direct field analyses, we have shown that there are substantial differences

523 in biomass and cell densities between green and red blooms. Additionally, the

524 initial FT-IR untargeted metabolic profiling revealed that there were

525 wavenumbers associated with protein/amino acids were more abundant in the

526 green blooms, whereas lipid and carbohydrate chemistry predominated in the red

527 blooms. Such differences in FT-IR spectra between the green and red

528 communities were similar to those detected by single-celled synchrotron-based

529 infrared spectroscopy of Arctic snow algae communities by Lutz *et al*. (2015),

530 who found that green communities were dominated by functional groups

531 associated with proteins and red communities by lipids.

532

533 ***Astaxanthin increase and chlorophyll content decrease in red blooms***

534 Snow surface pigmentation is a fundamental marker for identifying and

535 classifying snow algae communities during field campaigns and in research

536 based on satellite images (Fretwell *et al*., 2011). However, it cannot be assumed

537 that pigment composition does not vary between blooms, especially as the

538 species composition of the green and red communities have not been previously

539 described. We found that between green and red communities, although the

540 composition of the pigments was similar, the concentrations of each pigment was

541 not. Our pigment data for the Ryder Bay snow algal communities was consistent

542 with those of other snow algal blooms around the world. For example, Remias *et*

543 *al*. (2010, 2013) and Lutz *et al*. (2015, 2016) reported higher concentrations of

544   chlorophyll and xanthophyll cycle related compounds in green blooms, although,

545   unlike Remias *et al.* (2010), we were unable to detect α-tocopherol (vitamin E) in

546   the cells. The detected carotenoids potentially play a key role in energy

547   dissipation in chloroplasts under high light conditions (Demming-Adams &

548   Adams, 1996; Remias *et al.*, 2010). Higher concentrations of astaxanthin esters

549   in red blooms have also been reported elsewhere (Lutz *et al.*, 2015, Remias &

550   Lutz, 2007), the production of which can be dependent on developmental stage

551   (Holzinger *et al.*, 2016) or upon environmental stresses, in particular light intensity

552   and nutrient deficiency (Remias *et al.*, 2005, 2010; Lutz *et al.*, 2014; Minhas *et*

553   *al.*, 2016).

554

555   ***Concentrations of free fatty acids vary, but those of glycerolipids largely***

556   ***do not, between green and red blooms***

557   Our analyses with both untargeted and targeted metabolomic profiling

558   approaches (Bundy *et al.*, 2009) reveal many differences and similarities between

559   the green and red bloom communities and confirmed the field findings from the

560   FT-IR data. The lipid profiling showed that only the free fatty acid concentrations

561   differed between bloom types (with higher concentrations in the red

562   communities), and that the glycerolipid and fatty acid composition was similar

563   between blooms. Such profiles are characteristic of other snow algae blooms, in

564   which the high degree of fatty acid saturation is hypothesised to be related to

565   membrane stability at low temperatures (Bidigare *et al.*, 1993; Spijkerman *et al.*,

566   2012; Leya, 2013). Specifically, this is characteristic of *Chlamydomonas nivalis*

567   (Řezanka *et al.*, 2014), with Lukeš *et al.* (2014) relating the membrane lipid

568   composition to a broad thermal tolerance in terms of growth, electron transport

569   and oxygen evolution, compared to the temperate species *Chlamydomonas*

570   *reinhardtii*.

571

572   ***Distinct metabolic profiles of red and green snow algae communities***

573   The GC-MS profiling revealed that the dominant metabolites and metabolic

574   pathways in green blooms were associated with nitrogen and amino acid

575   metabolism, and in red blooms with osmolyte and fatty acid metabolism. High on

576   the list for compounds associated with green communities were lysine and its

577   precursor aminoadipic acid, which importantly is a precursor for penicillin

578   synthesis in fungi that produce α-aminoadipate (Fazius *et al.*, 2012). Also

579   dominant in the green blooms was calystegine, an alkaloid involved in plant-

580   bacterial communication, including with *Pseudomonas* (a reported bacterial

581   genus in our 16S sequencing), which is reported to catabolise it (Goldman *et al.*,

582   1996). Glycerol, sugar alcohols and other low molecular weight carbohydrates

583   have been reported previously in red snow algae, with their function associated

584   with osmotic acclimation (Eggert & Karston, 2010). Remias *et al.* (2013) also

585   detected high concentrations of glycerol and sugar alcohols in red blooms in

586   Antarctica. In contrast, studies of snow algal communities in the High Arctic by

587   Lutz *et al.* (2015) found that compounds related to purine and tryptophan

588   metabolism were more abundant in green communities than in red communities,

589   and were considered important in the increased growth rates of green blooms.

590   Although we detected metabolites in these pathways, they were not identified as

591   key determinants for either green or red blooms. This suggests that the

592   community composition and exudates could be functionally different between

593   Arctic and Antarctic sites. Such metabolic differences could be due to acclimation

594   effects or true adaptation to the local environment though more sites would need

595   to be studied before these hypotheses can be fully tested.

596

597   ***Snow algae community composition differs between bloom types but that***

598   ***of associated fungi and bacteria does not***

599   The algal cells in our study were structurally similar to snow algae cells described

600   in the Arctic (Svalbard) and North America (Hoham *et al.*, 1983; Müller *et al.*,

601   1998), with some red cells appearing morphologically similar to *Haematoccus*

602   *pluvialis* (Wayama *et al.*, 2013). The metabarcoding revealed that communities

603   were dominated by an unknown *Alveolata* (SAR), a yeast in the genus

604   *Cryptococcus* (*Tremellaceae*) and chytrids in the *Rhizophydiales* (Fungi) (Fig. **5**).

605   The latter are zoosporic fungi common in wet, cold habitats, which have been

606   widely reported in other snow algae blooms (Schmidt *et al.*, 2012; Naff *et al.*,

607   2013; Brown *et al.*, 2015; Comeau *et al.*, 2016; Seto and Degawa 2018). Within

608   the *Chlorophyta*, we were able to detect *Chlamydomonas*, *Chlorella*, uncultured
609   *Chloromonas* and two taxa assigned as unknown Chlorophyceae and unknown
610   Chlorophyta. Whether the Antarctic community contains endemic species
611   requires further study over a wider study area (Petz *et al*., 2007; De Wever *et al*.
612   2009). In this context, Remias *et al.* (2013), studying snow algal communities
613   from locations north (Goudier Island and Paradise Harbour, 64°S) of our location
614   (~68°S), determined species matching our metabarcoding OTUs for the red
615   blooms (*Chloromonas*), implying that this taxon may be distributed widely, at least
616   along the Antarctic Peninsula. In a similar study in continental Antarctica (Yatude
617   Valley, Langhovde at 69°S), Fujii *et al*. (2010) also identified a similar community
618   of *Chlorella*, *Chlamydomonas* and *Chloromonas* as well as other green algae
619   (*Raphydonema* and *Koliella*) and, as here, a range of yeasts. Although the
620   detailed composition of bacterial, protist and fungal communities in snow algal
621   blooms may be different across the globe, it is becoming apparent that snow
622   algae communities have similar wide functional and taxonomic structures. The
623   dominance of fungi, specifically yeasts and chytrids, in the communities studied
624   here is of particular note, with fungi also having been identified as important
625   components of Arctic snow packs (Maccario *et al*., 2014). Bacteria and fungi can
626   utilise simple and complex organic compounds within the snow pack (eg.
627   *Pseudomonas*, See-Too *et al*. (2016)) and numerous studies have reported
628   bacterial genera, such as *Polarmonas*, *Flavobacteria* and *Sphingobacteria*, living
629   in close association with *Chloromonas* and Chlamydomonadaceae (Hoham &
630   Duval, 2001; Komarek & Nedbalova, 2007; Hisakawa *et al*., 2015; Lutz *et al*.,
631   2015, 2016; Hamilton & Havig, 2017). There were also a large number of OTUs
632   that could not be assigned to a genus or species, implying that the communities
633   in the Antarctic snow packs are yet to be fully identified, characterised and
634   incorporated into public databases such as Silva (Quast et al., 2013).
635   Additionally, the diversity of the genetic, metabolic and growth phenotypes of a
636   wider spatial range of populations needs to be determined, to assess their
637   resilience to ongoing environmental changes and to predict future shifts in their
638   ranges. Whether the structure of these communities will be sufficiently resilient to
639   withstand abiotic parameters that are outside the normal range of their niche, as

640 a result of climate change, remains to be tested by resolving the phenotypic

641 plasticity of each species (Hoham, 1975; Morgan-Kiss *et al.*, 2006; Convey *et al.*,

642 2014; Rengefors *et al.*, 2015). Overall, such studies will contribute to

643 understanding the functional and taxonomic diversity of polar microbial

644 ecosystems (Keeling *et al.*, 2014; Cavicchioli, 2015) and the contribution of snow

645 algae to polar ecosystems and global carbon budgets.

646

659

660 **Author contributions**

661 MPD, KKN, PC, LSP designed and planned the field work and logistics. MPD

662 carried out the field work. MPD, LN and AGS planned the field sample analysis

663 at Rothera and Cambridge with MPD and LN extracting and analysing the

664 metabolites at Cambridge. MHO performed the DNA extraction for

665 metabarcoding and PS performed the metabarcoding bioinformatics. FB and

666 BKWL carried out the algae isolation and targeted 18S analysis. MPD and SS

667 carried out the pigment. MPD led the writing the manuscript with all other authors

668 contributing and editing text. All authors have seen and approved the final

669 version.

670

671

References

Altschul SF, Gish W, Miller W, Myers EW, Lipman DJ. 1990. Basic local alignment search tool. *Journal of Molecular Biology* **215**: 403-410.

Anderson MJ. 2001. A new method for non-parametric multivariate analysis of variance. *Austral Ecology* **26**: 32–46.

Anesio AM, Lutz S, Chrismas, NAM, Benning LG. 2017. The microbiome of glaciers and
ice sheets. *NPJ Biofilms and Microbiomes* **3**: 10

Anesio AM, Raiswell R, Edwards A, Newton RJ, Gill F, Benning LG. 2016. The biogeography of red snow microbiomes and their role in melting arctic glaciers. *Nature*. **7**: 11968.

Benning LG, Phoenix VR, Yee N, Tobin MJ. 2004. Molecular characterization of cyanobacterial silicification using synchrotron infrared micro-spectroscopy. *Geochimica et Cosmochimica Acta* **68**: 729–741.

Bidigare RR, Ondrusek ME. 1993. Evidence for a photoprotective function for secondary carotenoids of snow algae. *Journal of Phycology* **29**: 427-434.

Boetius A, Anesio AM, Deming JW, Mikucki JA, Rapp JZ. 2015. Microbial ecology of the cryosphere: sea ice and glacial habitats. *Nature Reviews: Microbiology* **13**: 677-690.

Broady PA. 1996. Diversity, distribution and dispersal of Antarctic terrestrial algae. *Biodiversity and Conservation* **5**: 1307-1335.

702 **Brown SP, Olson BJSC, Jumpponen A. 2015.** Fungi and Algae Co-Occur in
703 Snow: An Issue of Shared Habitat or Algal Facilitation of Heterotrophs? *Arctic,*
704 *Antarctic, and Alpine Research*. **47**: 729-749.

705

706 **Brunetti C, George RM, Tattini M, Field K, Davey MP. 2013.** Metabolomics in
707 plant environmental physiology. *Journal of Experimental Botany* **64**: 4011–4020.

708

709 **Bundy JG, Davey MP, Viant MR. 2009.** Environmental metabolomics: a critical
710 review and future perspectives. *Metabolomics* **5**: 3-21.

711

712 **Burton-Johnson A, Black M, Fretwell PT, Kaluza-Gilbert J. 2016.** An
713 automated methodology for differentiating rock from snow, clouds and sea in
714 Antarctica from Landsat 8 imagery: a new rock outcrop map and area estimation
715 for the entire Antarctic continent. *The Cryosphere* **10**: 1665-1677.

716

717 **Callahan BJ, McMurdie PJ, Rosen MJ, Han AW, Johnson AJA, Holmes SP.**
718 **2016.** DADA2: high-resolution sample inference from Illumina amplicon data.
719 *Nature Methods* **13**: 581–583.

720

721 **Caporaso JG, Kuczynski J, Stombaugh J, Bittinger K, Bushman FD,**
722 **Costello EK, Fierer N, Pena AG, Goodrich JK, Gordon JI, et al. 2010.** QIIME
723 allows analysis of high-throughput community sequencing data. *Nature Methods*
724 **7**: 335–336.

725

726 **Cavicchioli R. 2015.** Microbial ecology of Antarctic aquatic systems. *Nature*
727 *Reviews: Microbiology* **13**: 691-706.

728

729 **Chong J, Soufan O, Li C, Caraus I, Li S, Bourque G, Wishart DS, Xia J. 2018.**
730 MetaboAnalyst 4.0: towards more transparent and integrative metabolomics
731 analysis. *Nucleic Acids Research* **46(W1)**: W486-W494.

732

733 **Chong j, Xia J. 2018.** MetaboAnalystR: an R package for flexible and

734   reproducible analysis of metabolomics data. *Bioinformatics* **1–2**: doi:
735   10.1093/bioinformatics/bty528
736

737   **Chown SL, Convey P. 2012.** Spatial and temporal variability in terrestrial
738   Antarctic biodiversity. In: Rogers AD, Johnston NM, Murphy EJ, Clarke A, eds.
739   *Antarctic Ecosystems: An Extreme Environment in a Changing World.*
740   Chichester, UK: Blackwell Publishing Ltd., 13-43.
741

742   **Comeau AM, Vincent WF, Bernier L, Lovejoy C. 2016.** Novel chytrid lineages
743   dominate fungal sequences in diverse marine and freshwater habitats. *Science*
744   *Reports*. **6**: 30120
745

746   **Convey P. 2017.** *Antarctic Biodiversity. Reference Module in Life Sciences.*
747   Elsevier. [WWW document] URL https://doi.org/10.1016/B978-0-12-809633-
748   8.02182-8. [accessed 09 January 2019].
749

750   **Convey P. 2011.** Antarctic terrestrial biodiversity in a changing world. *Polar*
751   *Biology* **34**: 1629-1641.
752

753   **Convey P, Chown SL, Clarke A, Barnes DKA, Bokhorst S, Cummings V,**
754   **Ducklow HW, Frati F, Green TGA, et al. 2014.** The spatial structure of Antarctic
755   biodiversity. *Ecological Monographs* **84**: 203–244.
756

757   **Cook JM, Hodson AJ, Taggart AJ, Mernild SH, Tranter M. 2017.** A predictive
758   model for the spectral "bioalbedo" of snow. *Journal of Geophysical Research:*
759   *Earth Surface* **122**: 434–454.
760

761   **Davey MP, Burrell MM, Woodward FI, Quick WP. 2008.** Population specific
762   metabolic phenotypes of *Arabidopsis lyrata* ssp. *petraea*. *New Phytologist* **177**:
763   380-388.
764

765   **Davey MP, Duong GH, Tomsett E, Litvinenko ACP, Howe CJ, Horst I, Smith**
766   **AG. 2014.** Triacylglyceride production and autophagous responses in
767   *Chlamydomonas reinhardtii* depend on resource allocation and carbon source.
768   *Eukaryotic Cell* **13**: 392-400.

770   **Demmig-Adams B, Adams WW. 1996.** The role of xanthophyll cycle
771   carotenoids in the protection of photosynthesis. *Trends in Plant Science* **1**: 21-
772   26.

774   **De Wever A, Leliaert F, Verleyen E, Vanormelingen P, Van der Gucht K,**
775   **Hodgson DA, Sabbe K, Vyverman W. 2009.** Hidden levels of phylodiversity in
776   Antarctic green algae: further evidence for the existence of glacial refugia.
777   *Proceedings of the Royal Society B*. **276**: 3591-3599.

779   **Dierssen HM, Smith RC, Vernet M. 2002.** Glacial meltwater dynamics in coastal
780   waters west of the Antarctic Peninsula. *PNAS* **99**: 1790-1795.

782   **Dunn WB, Broadhurst D, Begley P, Zelena E, Francis-McIntyre S, Anderson**
783   **N, Brown M, Knowles JD, Halsall A, Haselden JN, et al. 2011.** Procedures for
784   large-scale metabolic profiling of serum and plasma using gas chromatography
785   and liquid chromatography coupled to mass spectrometry. *Nature Protocols* **6**:
786   1060–1083.

788   **Eggert A, Karsten U. 2010.** Low Molecular Weight Carbohydrates in Red Algae
789   – an Ecophysiological and Biochemical Perspective. In: Seckbach J, Chapman
790   D, eds. *Cellular Origin, Life in Extreme Habitats and Astrobiology: Red Algae in*
791   *the Genomics Age*. Dordrecht, Netherlands: Springer Science and Business
792   Media, V13 443-456.

794   **Fazius F, Shelest E, Gebhardt P, Brock M. 2012.** The fungal α-aminoadipate
795   pathway for lysine biosynthesis requires two enzymes of the aconitase family for

796 the isomerization of homocitrate to homoisocitrate. *Molecular Microbiology* **86**:
797 1508–1530.
798
799 **Fogg GE. 1976.** Observations on the snow algae of the South Orkney Islands.
800 *Philosophical Transactions of the Royal Society B.* **252**: 279-287.
801
802 **Fretwell PT, Convey P, Fleming AH, Peat HJ, Hughes KA. 2011.** Detecting
803 and mapping vegetation distribution on the Antarctic Peninsula from remote
804 sensing data. *Polar Biology* **34**: 273–281.
805
806 **Fujii M, Takano Y, Kojima H, Hoshino T, Tanaka R, Fukui M. 2010.** Microbial
807 community structure, pigment composition, and nitrogen source of red snow in
808 Antarctica. *Microbial Ecology* **59**:466–475.
809
810 **Ganey GQ, Loso MG, Bryant Burgess A, Dial RJ. 2017.** The role of microbes
811 in snowmelt and radiative forcing on an Alaskan icefield. *Nature Geoscience* **10**:
812 754-759.
813
814 **Goldmann A, Message B, Tepfer D, Molyneux RJ, Duclos O, Boyer FD, Pan
815 YT, Elbein AD. 1996.** Biological activities of the nortropane alkaloid, calystegine
816 B$_2$, and analogs: Structure-Function Relationships. *Journal of Natural Products*
817 **59**: 1137-1142.
818
819 **Hamilton TL, Havig J. 2017.** Primary productivity of snow algae communities on
820 stratovolcanoes of the Pacific Northwest. *Geobiology*. **15**: 280–295.
821
822 **Hisakawa N, Quistad SD, Hester ER, Martynova D, Maughan H, Sala E,
823 Gavrilo MV, Rohwer F. 2015.** Metagenomic and satellite analyses of red snow
824 in the Russian Arctic. *PeerJ* 3:e1491 https://doi.org/10.7717/peerj.1491
825

826 **Hodson A, Anesio AM, Tranter M, Fountain A, Osborn M, Priscu J,**

827 **Laybourn-Parry J, Sattler B. 2008.** Glacial Ecosystems. *Ecological*

828 *Monographs.* **78**: 41-67.

829

830 **Hoham RW. 1975.** Optimum temperatures and temperature ranges for growth of

831 snow algae. *Arctic and Alpine Research* **7**: 13-24.

832

833 **Hoham RW, Duval B. 2001.** Microbial ecology of snow and freshwater ice with

834 emphasis on snow algae. In: Jones HG, Pomeroy JW, Walker DA, Hoham RW,

835 eds. *Snow ecology: An interdisciplinary examination of snow-covered*

836 *ecosystems*. Cambridge, UK: Cambridge University Press, 168-228.

837

838 **Hoham RW, Mullet JE, Roemer SC. 1983.** The life history and ecology of the

839 snow alga *Chloromonas polyptera* comb. nov. (Chlorophyta, Volvocales).

840 *Canadian Journal of Botany* **61**: 2416-2429.

841

842 **Holzinger A, Allen MC, Dimitri DD. 2016.** Hyperspectral imaging of snow algae

843 and green algae from aeroterrestrial habitats. *Journal of Photochemistry &*

844 *Photobiology, B: Biology* **162**: 412–420.

845

846 **Inskeep WP, Bloom PR. 1985.** Extinction coefficients of chlorophyll-*a* and

847 chlorophyll-*b* in n,n-dimethylformamide and 80-percent acetone. *Plant*

848 *Physiology* **77**: 483-485.

849

850 **Keeling PJ, Burki F, Wilcox HM, Allam B, Allen EE, Amaral-Zettler LA,**

851 **Armbrust EV, Archibald JM, Bharti AK, Bell CJ, et al. 2014.** The Marine

852 Microbial Eukaryote Transcriptome Sequencing Project (MMETSP): Illuminating

853 the functional diversity of eukaryotic life in the oceans through transcriptome

854 sequencing. *PLOS Biology* **12**: e1001889

855

856   **Komárek J, Nedbalová L. 2007.** Green Cryosestic Algae. In: Seckbach J, ed.
857   *Algae and Cyanobacteria in Extreme Environments*. Dordrecht, Netherlands:
858   Springer, 321–342.
859
860   **Leya T. 2013.** Snow Algae: Adaptation Strategies to Survive on Snow and Ice.
861   In: Seckbach J, Oren A, Stan-Lotter H, eds. *Polyextremophiles. Cellular Origin,*
862   *Life in Extreme Habitats and Astrobiology, vol 27*. Dordrecht, NL: Springer, 401-
863   423.
864
865   **Lukeš M, Procházková L, Shmidt V, Nedbalová L, Kaftan D. 2014.**
866   Temperature dependence of photosynthesis and thylakoid lipid composition in
867   the red snow alga *Chlamydomonas* cf. *nivalis* (Chlorophyceae). *FEMS*
868   *Microbiological Ecology* **89**: 303–315.
869
870   **Lutz S, Anesio AM, Edwards R, Benning LG. 2016.** Linking microbial diversity
871   and functionality of arctic glacial surface habitats. *Environmental Microbiology* **19**:
872   551–565.
873
874   **Lutz S, Anesio AM, Field K, Benning LG. 2015.** Integrated 'Omics', Targeted
875   metabolite and single-cell analyses of Arctic snow algae functionality and
876   adaptability. *Frontiers in Microbiology* **6**: 1323 doi:10.3389/fmicb.2015.01323
877
878   **Lutz S, Anesio AM, Jorge Villar SE, Benning LG. 2014.** Variations of algal
879   communities cause darkening of a Greenland glacier. *FEMS Microbiological*
880   *Ecology* **89**: 402–414.
881
882   **Maccario L, Vogel TM, Larose C. 2014.** Potential drivers of microbial community
883   structure and function in Arctic spring snow. *Frontiers in Microbiology*. **5**: Article
884   413 doi: 10.3389/fmicb.2014.00413
885

New Phytologist

886 **Mayers JJ, Flynn KJ, Shields RJ. 2013.** Rapid determination of bulk microalgal
887 biochemical composition by Fourier Transform Infrared Spectroscopy.
888 *Bioresource* Technology **148**: 215-220.

889

890 **Minhas AK, Hodgson P, Barrow CJ, Adholeya A. 2016.** A review on the
891 assessment of stress conditions for simultaneous production of microalgal lipids
892 and carotenoids. *Frontiers in Microbiology* **7**: 546 doi: 10.3389/fmicb.2016.00546

893

894 **Morgan-Kiss RM, Priscu JC, Pocock T, Gudynaite-Savitch L, Huner NPA.**
895 **2006.** Adaptation and acclimation of photosynthetic microorganisms to
896 permanently cold environments. *Microbiology and Molecular Biology Reviews* **70**:
897 222–252.

898

899 **Müller T, Bleiβ W, Martin CD, Rogaschewski S, Fuhr G. 1998.** Snow algae
900 from northwest Svalbard: their identification, distribution, pigment and nutrient
901 content. *Polar Biology* **20:** 14-32.

902

903 **Naff CS, Darcy JL, Schmidt SK. 2013.** Phylogeny and biogeography of an
904 uncultured clade of snow chytrids. *Environmental Microbiology*. **15:** 2672–2680.

905

906 **Paliy O, Shankar V. 2016.** Application of multivariate statistical techniques in
907 microbial ecology. *Molecular Ecology* **25**: 1032–1057.

908

909 **Petz W, Valbonesi A, Schiftner U, Quesada A, Cynan Ellis-Evans J. 2017.**
910 Ciliate biogeography in Antarctic and Arctic freshwater ecosystems: endemism
911 or global distribution of species? *FEMS Microbiological Ecology* **59**: 396–408.

912

913 **Quast C, Pruesse E, Yilmaz P, Gerken J, Schweer T, Yarza P, Peplies J,**
914 **Glöckner FO. 2013.** The SILVA ribosomal RNA gene database project: improved
915 data processing and web-based tools. *Nucleic Acids Research* **41(D1)**: D590-
916 D596.

917

918 **Remias D, Albert A, Lütz C. 2010.** Effects of realistically simulated, elevated UV

919 irradiation on photosynthesis and pigment composition of the alpine snow alga

920 *Chlamydomonas nivalis* and the Arctic soil alga *Tetracystis* sp. (Chlorophyceae).

921 *Photosynthetica* **48**: 269-277.

922

923 **Remias D, Lütz C. 2007.** Characterisation of esterified secondary carotenoids

924 and of their isomers in green algae: a HPLC approach. *Algological Studies* **124**:

925 85–94.

926

927 **Remias D, Lütz-Meindl U, Lütz C. 2005.** Photosynthesis, pigments and

928 ultrastructure of the alpine snow alga *Chlamydomonas nivalis*. European *Journal*

929 *of Phycology* **40**: 259–268.

930

931 **Remias D, Wastian H, Lütz C, Leya T. 2013.** Insights into the biology and

932 phylogeny of *Chloromonas polyptera* (Chlorophyta), an alga causing orange

933 snow in Maritime Antarctica. *Antarctic Science* **25**: 648-656.

934

935 **Rengefors K, Logares R, Laybourn-Parry J, Gast RJ. 2015.** Evidence of

936 concurrent local adaptation and high phenotypic plasticity in a polar

937 microeukaryote. *Environmental Microbiology* **17**: 1510–1519.

938

939 **Řezanka T, Nedbalová L, Procházková L, Sigler K. 2014.** Lipidomic profiling

940 of snow algae by ESI-MS and silver-LC/APCI-MS. *Phytochemistry* **100**: 34–42.

941

942 **Rintoul SR, Chown SL, De Conto RM, England MH, Fricker HA, Masson-**

943 **Delmotte V, Naish TR, Siegert MJ, Xavier JC. 2018.** Choosing the future of

944 Antarctica. *Nature* **558**: 233-241.

945

946 **Rogers AD, Clarke A, Johnston NM, Murphy EJ. 2007.** Introduction. Antarctic

947 ecology from genes to ecosystems: the impact of climate change and the

948 importance of scale. *Philosophical Transactions of the Royal Society B.* **362**: 5–

949 9.

950

951 **Schmidt SK, Naff CS, Lynch RC. 2012.** Fungal communities at the edge:
952 ecological lessons from high alpine fungi. *Fungal Ecology* **5**: 443–452.

953

954 **See-Too WS, Lima, Ee R, Convey P, Pearce DA, Yin WF, Chan KG. 2016.**
955 Complete genome of *Pseudomonas* sp. strain L10.10, a psychrotolerant
956 biofertilizer that could promote plant growth. *Journal of Biotechnology* **222:** 84–
957 85.

958

959 **Seto k, Degawa y. 2018.** *Collimyces mutans* gen. et sp. nov. (Rhizophydiales,
960 Collimycetaceae fam. nov.), a new chytrid parasite of *Microglena* (Volvocales,
961 clade Monadinia). *Protist* **169:** 507–520.

962

963 **Spijkerman E, Wacker A, Weithoff G, Leya T. 2012.** Elemental and fatty acid
964 composition of snow algae in Arctic habitats. *Frontiers in Microbiology* **3**: 390.

965

966 **Stibal M, Box JE, Cameron KA, Langen PL, Yallop ML, Mottram RH, Khan**
967 **AL, Molotch NP, Chrismas NAM et al. 2017.** Algae drive enhanced darkening
968 of bare ice on the Greenland ice sheet. *Geophysical Research Letters* **44**:
969 https://doi.org/
970 10.1002/2017GL075958

971

972 **Turner J, Bindschadler R, Convey P, di Prisco G, Fahrbach E, Gutt J,**
973 **Hodgson D, Mayewski P, Summerhayes C. 2009.** *Antarctic Climate Change*
974 *and the Environment.* Scientific Committee on Antarctic Research: Cambridge
975 526 pp.

976

977 **Turner J, Lu H, White I, King JC, Phillips T, Hosking JS, Bracegirdle TJ,**
978 **Marshall GJ, Mulvaney R, Deb P. 2016.** Absence of 21st century warming on
979 Antarctic Peninsula consistent with natural variability. *Nature* **535**: 411–415.

980

981 **Vaughan DG. 2006.** Recent trends in melting conditions on the Antarctic
982 Peninsula and their implications of ice-sheet mass balance and sea level. Arctic,
983 Antarctic, and Alpine Research **38**: 147–152.
984
985 **Vyverman W, Verleyen E, Wilmotte A, Hodgson DA, Willems A, Peeters K,**
986 **Van de Vijver B, De Wever A, Leliaert F, Sabbe K. 2010.** Evidence for
987 widespread endemism among Antarctic micro-organisms. *Polar Science* **4**: 103-
988 113.
989
990 **Wang Y, Tian RM, Gao ZM, Bougouffa S, Qian PY. 2014.** Optimal eukaryotic
991 18S and universal 16S/18S ribosomal RNA primers and their application in a
992 study of symbiosis. *PLoS ONE* **9(3)**: e90053.
993 https://doi.org/10.1371/journal.pone.0090053
994
995 **Wayama M, Ota S, Matsuura H, Nango N, Hirata A, Kawano S. 2013.** Three-
996 dimensional ultrastructural study of oil and astaxanthin accumulation during
997 encystment in the green alga *Haematococcus pluvialis*. *PLoS ONE* **8**: e53618.
998 doi:10.1371/journal.pone.0053618
999
1000 **Wellburn AR. 1994.** The spectral determination of chlorophyll-*a* and
1001 chlorophhyll-*b*, as well as total carotenoids, using various solvents with
1002 spectrophotometers of different resolution. *Journal of Plant Physiology* **144**: 307-
1003 313.
1004
1005 **Williams WE, Gorton HL, Vogelmann TC. 2003.** Surface gas-exchange
1006 processes of snow algae. *PNAS* **100**: 562-566.
1007
1008
1009
1010
1011
1012

1013

1014　**Table 1.** Pigment composition of snow algae. Pigments expressed as mg g^{-1} dry

1015　cell mass from green and red snow algal communities collected from four

1016　locations in the maritime Antarctic (Rothera Point, Anchorage Island, Léonie

1017　Island and Lagoon Island) during austral summer (Jan–Feb) 2015. Data were

1018　pooled from all collection sites (mean ± SE, n = 6). Dominant pigments are

1019　highlighted in bold. * = $P ≤ 0.05$ between green and red communities. Arrows

1020　show trend of change from green to red communities.

1021

Pigment		Green community mg g^{-1} DCM	Red community mg g^{-1} DCM
Chlorophyll *a*	↓	3.37 (1.24)	0.28 (0.11) *
Chlorophyll *b*	↓	1.54 (0.47)	0.13 (0.06) *
Chlorophyll-like	↓	1.59 (0.66)	0.00 (0.00) *
β-Carotene	↓	0.40 (0.16)	0.00 (0.00) *
β-Carotene-like	↓	0.02 (0.02)	0.00 (0.00)
Lutein	↓	0.58 (0.19)	0.01 (0.01) *
Xanthophyll	↓	0.21 (0.07)	0.06 (0.03)
Astaxanthin-like	↑	0.03 (0.02)	0.07 (0.02)
Astaxanthin esters	↑	0.34 (0.13)	0.63 (0.30)

1023 ***Figure Legends:***

1024

1025 **Figure 1:** Representative image of snow algal blooms (red dominant foreground, green

1026 dominant midground) in January 2015 on Léonie Island, Ryder Bay, Antarctic Peninsula

1027 (See Supporting Information Table S1 for details). Note person in midground for scale.

1028

1029 **Figure 2**: Metabolic fingerprinting (FT-IR) reveals differences between green and red

1030 blooms. Score scatter plot (**a**) from principal component analysis of FT-IR wavenumber

1031 intensities of green (circles, *n* = 30) and red (squares, *n* = 40) snow algae communities

1032 collected from four locations adjacent to the Antarctic Peninsula (Rothera Point (RP),

1033 Anchorage Island (AN), Léonie Island (LE) and Lagoon Island (LA)) during January and

1034 February 2015 (austral summer). The score contribution plot (**b**) indicates which FT-IR

1035 wavenumbers differ the most between green (protein, amide I, II) and red (lipids, lipid esters,

1036 polysaccharides) snow algae communities along PC1 and PC2.

1037

1038 **Figure 3:** Lipid content of snow algae blooms. Total TAGs, membrane lipids and free fatty

1039 acids (as C16 equivalent) expressed as both mg g^{-1} dry cell mass (DCM; panels **a**, **c** and **e**)

1040 and mg l^{-1} snow melt (panels **b**, **d** and **f**) from green and red snow algae communities

1041 collected from four locations adjacent to the Antarctic Peninsula (Rothera Point, Anchorage

1042 Island, Léonie Island and Lagoon Island) during January and February 2015 (austral

1043 summer). Data are mean ± SD. Total green, red sample sizes (*n*) are: RP 4,3; AN 3,7; LE

1044 1,2; LG 3,3. Statistical differences (ANOVA) between green and red communities within a

1045 location are denoted by * = *P* ≤ 0.05, ** = *P* ≤ 0.01, *** = *P* ≤ 0.001.

1046

1047 **Figure 4**: Metabolic profiling (GC-MS) reveals differences between green and red blooms.

1048 Score scatter plot (**a**) from principal component analysis of putatively identified metabolite

1049 intensities (GC-MS) of green (circles, *n* = 11) and red (squares, *n* = 14) snow algae

1050 communities collected from four locations adjacent to the Antarctic Peninsula (Rothera Point

1051 (RP), Anchorage Island (AN), Léonie Island (LE) and Lagoon Island (LA)) during January

1052 and February 2015 (austral summer). The score contribution plot (**b**) values (top 20) are

1053 ranked in order of importance and are positive if they contribute towards PCA loading plots

1054 for the green snow algae communities and negative if they contribute towards the red snow

1055 algae communities. The full list of metabolites is presented in Supplementary Table **S4**.

1056

1057 **Figure 5**: Taxonomic composition of snow algae blooms. Percent contribution of taxonomic

1058 assignments for 99% aligned OTUs for 16S SSU rRNA and 18S ITS1 sequences in green

1059 and red snow algae communities from Ryder Bay, Antarctica during January and February

1060 2015 (austral summer). Percent contribution values are the mean relative abundance of the

1061 taxa in percentage of total sequences with more than 0.5% abundance and are classified at

1062 the class (**a**,**b**) or genus level (**c**,**d**). Low abundance OTU values are the sum of the

1063 percentages for taxa identified below 0.5% contribution. All values are mean of $n = 5$ (green

1064 community sites) or $n = 6$ (red community sites). SAR = "stramenopiles, alveolata, rhizaria".

1065 Detailed OTU read numbers, percent contributions and statistics are presented in

1066 **Supplementary Tables 6-8**.

1067
1068
1069
1070
1071
1072
1073
1074
1075
1076
1077

1078   ***Supporting Information:***

1079

1080   **Figure S1:** Alpha diversity rarefaction plots

1081   **Figure S2:** Snow algae community biomass and cell counts

1082   **Figure S3:** Representative UV-Vis absorption spectra of solvent ethanol extracts from green

1083   or red dominant snow algae communities

1084   **Figure S4:** Pigment content of snow algae blooms.

1085   **Figure S5:** Alpha diversity boxplots

1086   **Figure S6:** Screen shots of beta diversity boxplots

1087   **Figure S7:** Metabarcoding NMDS plots

1088   **Figure S8:** Composition of Chlorophyta OTUs in green and red snow algae blooms.

1089

1090   **Table S1:** Sampling locations and light (PAR) and temperatures recorded at snow surface

1091   and 5 cm depth during sampling.

1092   **Table S2.** FT-IR metabolic fingerprinting of snow algae communities.

1093   **Table S3.** Fatty acid composition of snow algae.

1094   **Table S4.** Score contribution of putatively identified metabolites associated with either

1095   green or red snow algae communities.

1096   **Table S5.** Metabolite pathways of the putatively identified metabolites associated with

1097   either green or red snow algae communities.

1098   **Table S6.** Percentage contributions and number of taxonomic assignments for **Level 2**

1099   **(Kingdom/Phylum)** 16S rRNA gene and ITS sequences in green and red snow algae

1100   communities.

1101   **Table S7.** Percentage contributions and number of taxonomic assignments for **Level 3**

1102   **(Order, Class)** 16S rRNA gene and ITS sequences in green and red snow algae

1103   communities.

1104   **Table S8.** Percentage contributions and numbers of taxonomic assignments for **Level 6**

1105   **(Family, Genus)** 16S rRNA gene and ITS sequences in green and red snow algae

1106   communities.

1107   **Table S9.** Targeted genomic identification of snow algae.

1108

1109   **Methods S1.** Raw read metabarcoding R script files in vegan.

1110

Figure 1

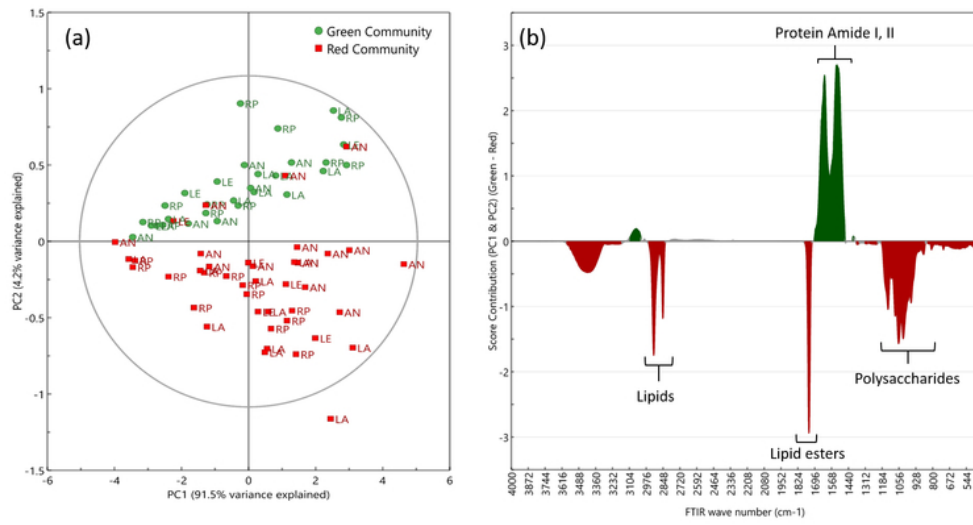219x146mm (300 x 300 DPI)

Figure 2
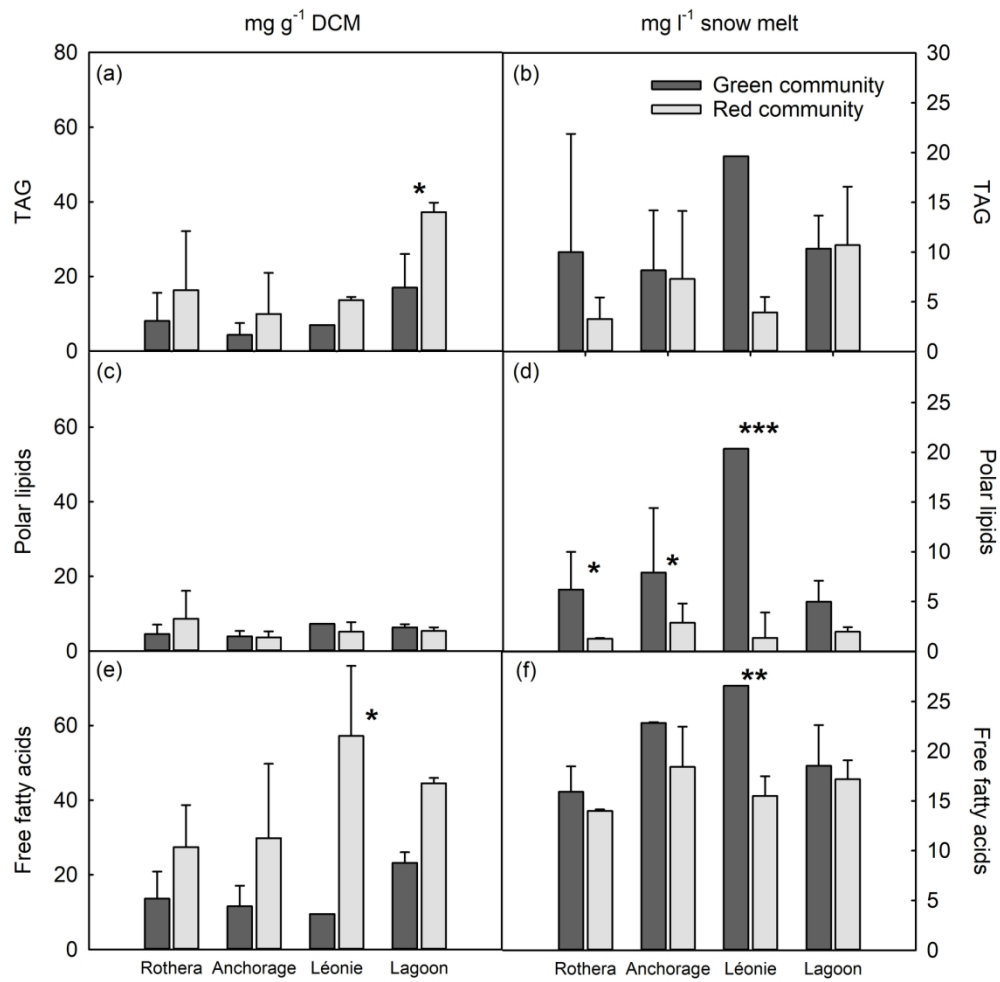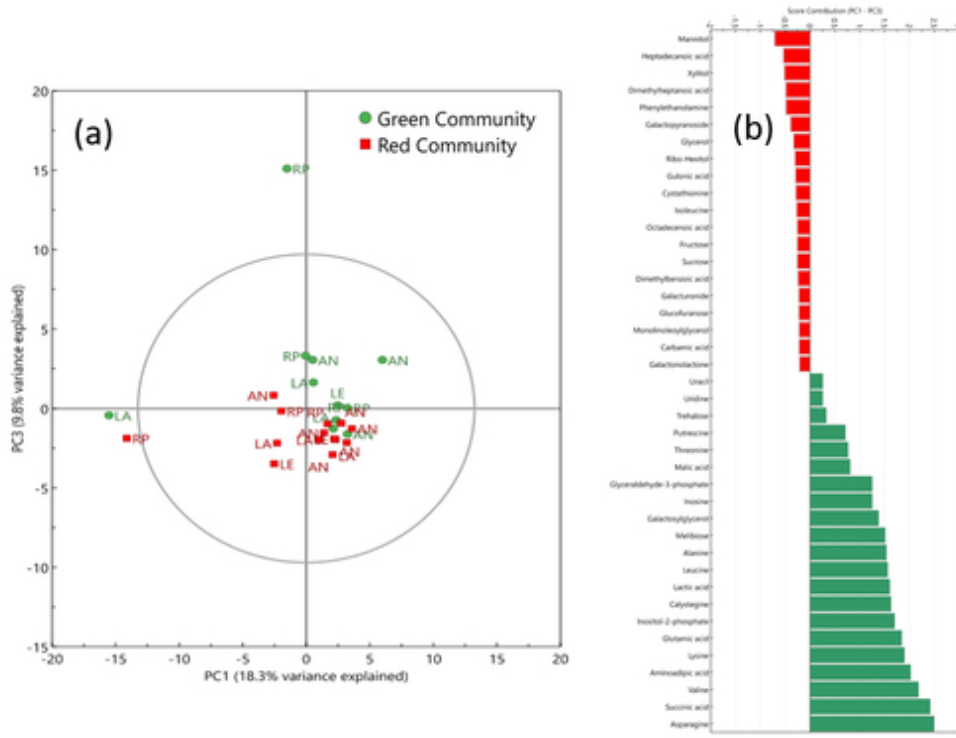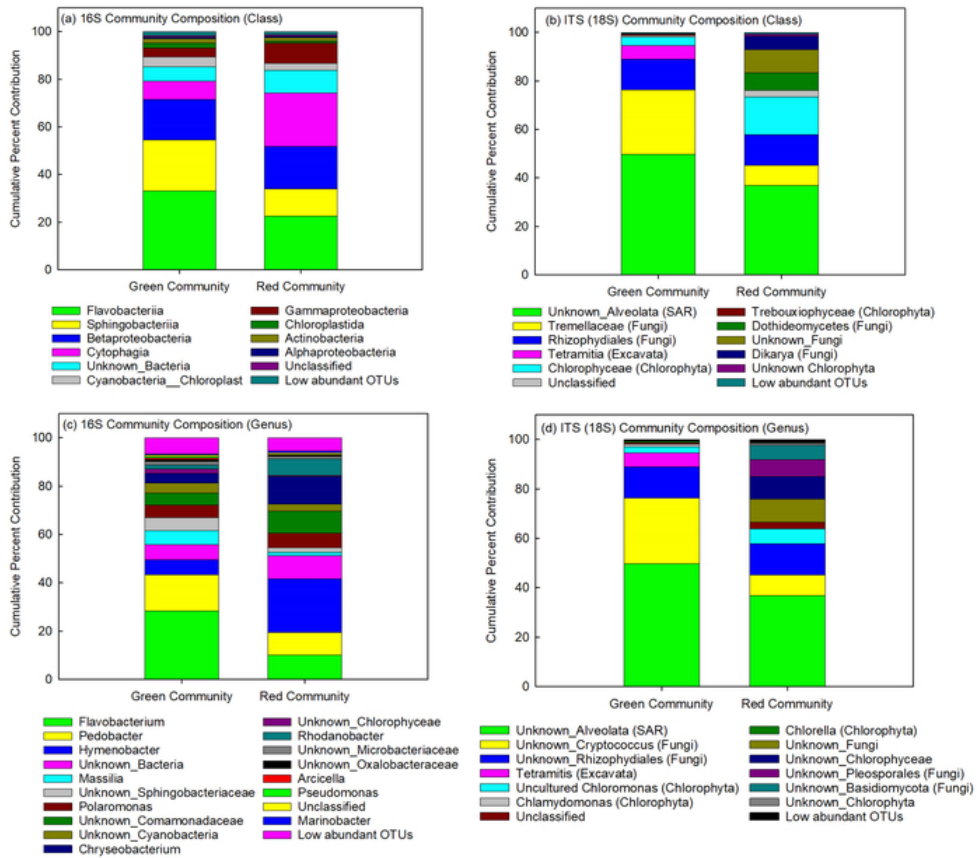
64x35mm (300 x 300 DPI)

Figure 3

161x161mm (300 x 300 DPI)

Figure 4

42x33mm (300 x 300 DPI)

Figure 5

60x54mm (300 x 300 DPI)